Electronic Supplementary Information (ESI)

p-i-n Silicon Nanowire Array-NGQD: A Metal-Free Electrocatalyst for Photoelectrochemical Hydrogen Evolution

Sk Riyajuddin, Sushil Kumar, Damini Badhwar, Shumile Ahmed Siddiqui, Jenifar Sultana and Kaushik Ghosh*

Institute of Nano Science & Technology, Knowledge City, Sector-81, SAS Nagar, Manauli P.O-140306, Mohali, Punjab, India

Correspondence author's email: kaushik@inst.ac.in

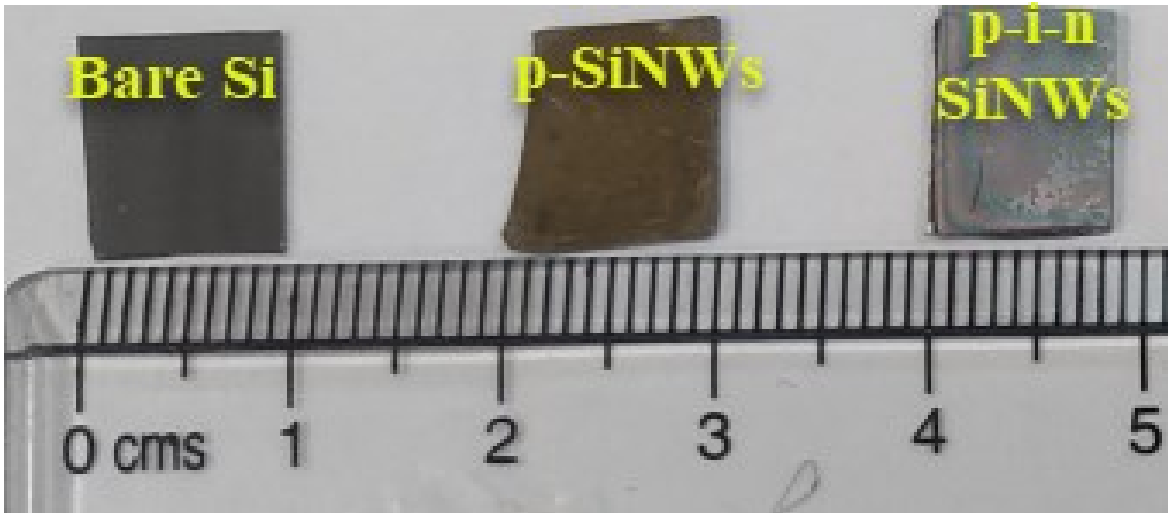

Fig. S1 The optical photograph of bare Si, p-SiNWs, and p-i-n SiNWs which have been further utilized for the fabrication of Photocathodes having a dimension of ~ (1x1) cm^2.

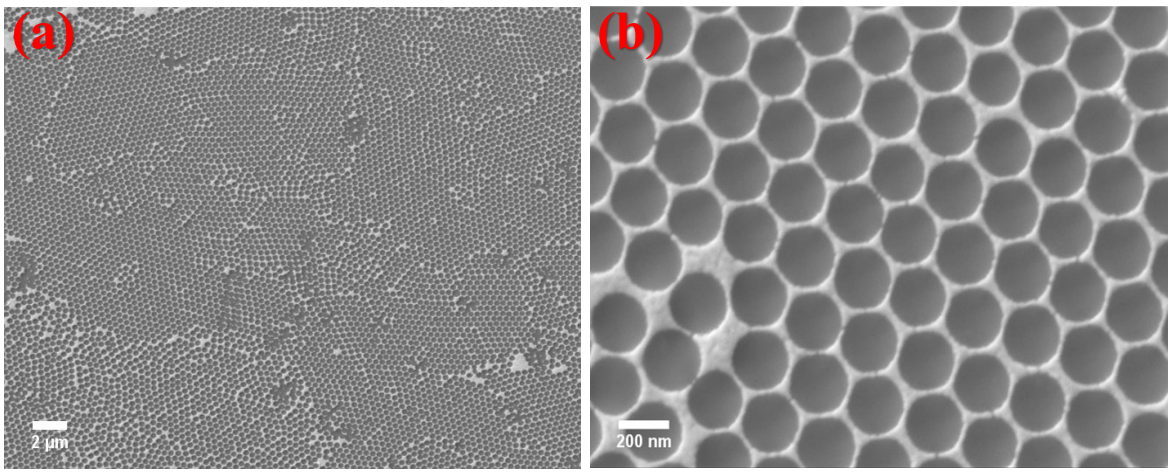

Fig. S2 FE-SEM images of (a)-(b) hexagonal honeycomb-like gold mesh arrays after removal of PS beads by mild sonication in Chloroform medium on the planar p-Si surface under low (2 µm scale) and high resolution (200 nm scale), respectively. The approximate size of these nanoholes are in the range of 240-250 nm.

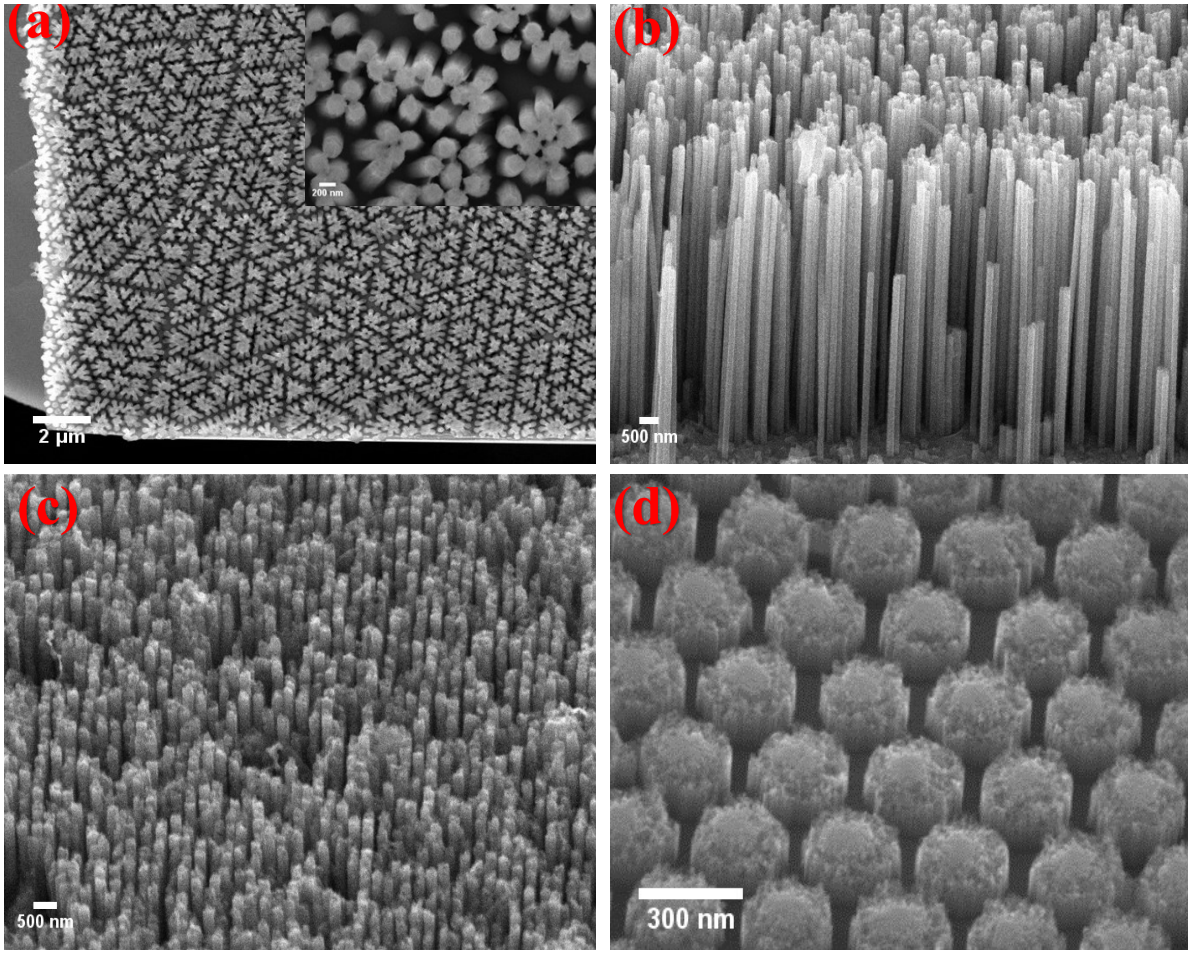

Fig. S3 FE-SEM image p-SiNWs obtain *via* different HF etching times of (a) 20 minutes, (b) 15 minutes, (c)10 minutes and (d) 1 minute, respectively. The 20 minutes etching results in the formation of ~ 10 µm long SiNWs which are collapsed with each other due to high capillary effect under solvent drying condition, shown as an inset of (a).

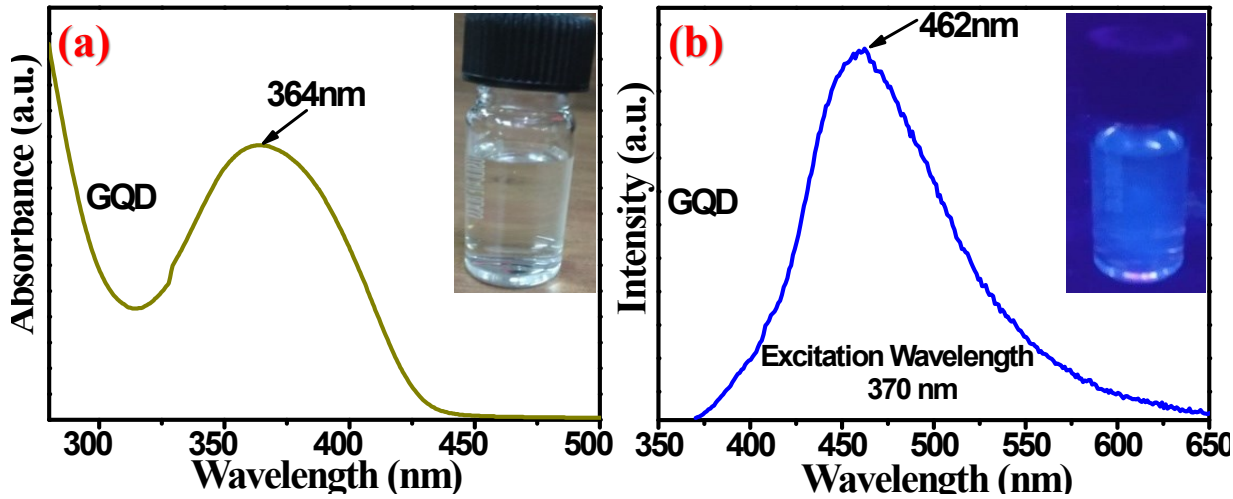

Fig. S4 (a) Absorbance spectra and (b) PL Spectra of GQD at an excitation wavelength of 340 nm.

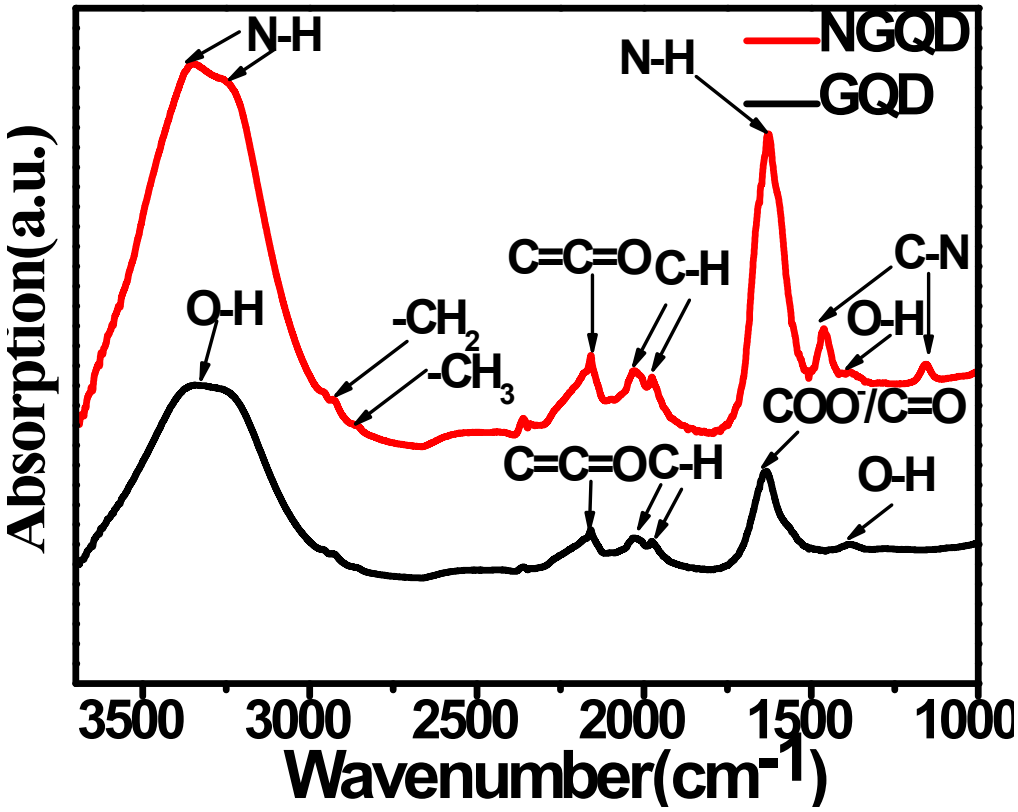

Fig. S5 ATR-FTIR absorption spectrum of GQD and NGQD.

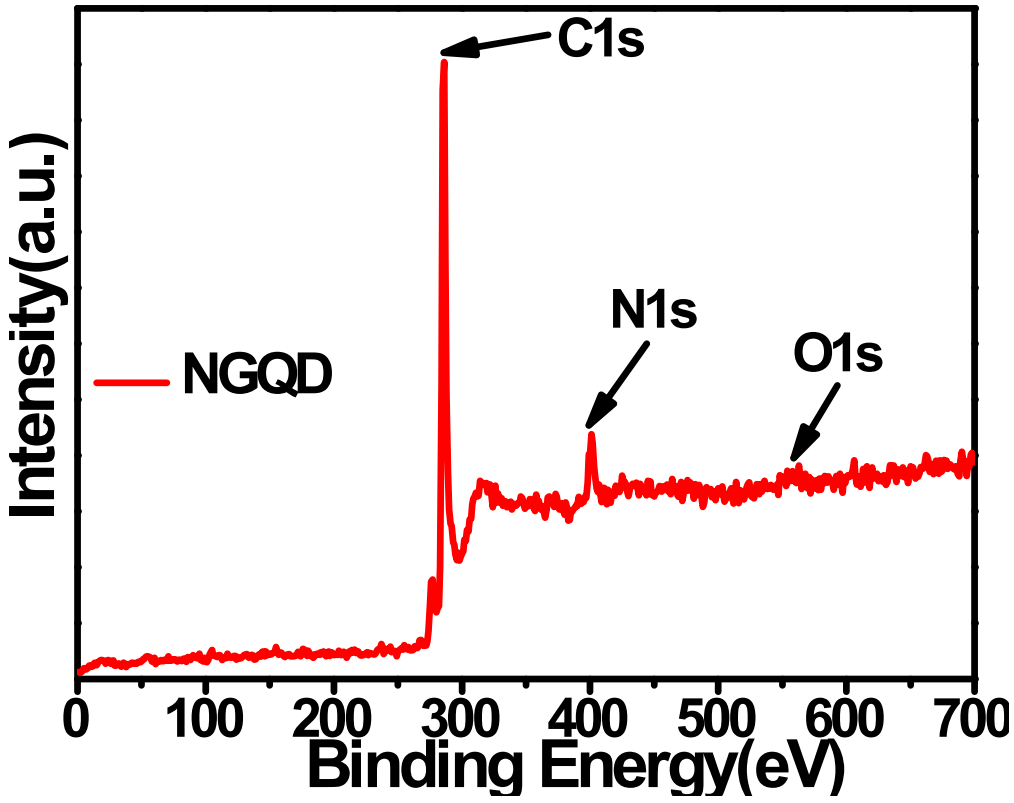

Fig. S6 XPS survey spectrum of as-prepared NGQD.

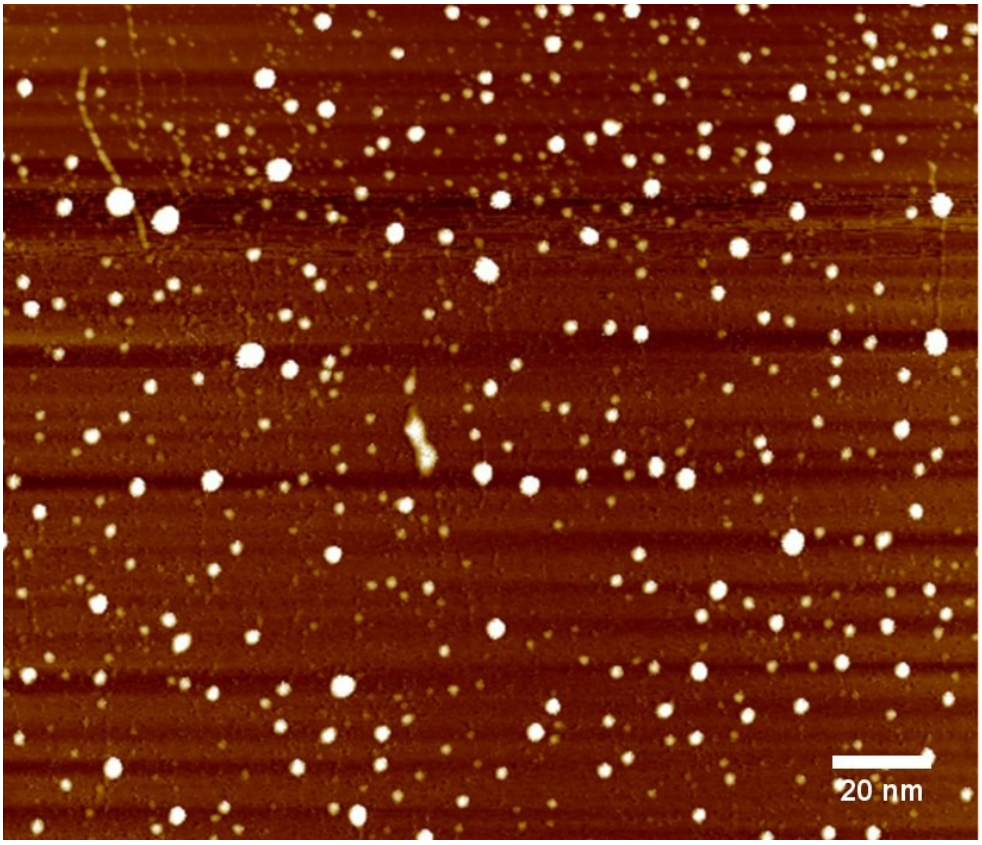

Fig. S7 Atomic Force Microscopy (AFM) image of as-prepared NGQD.

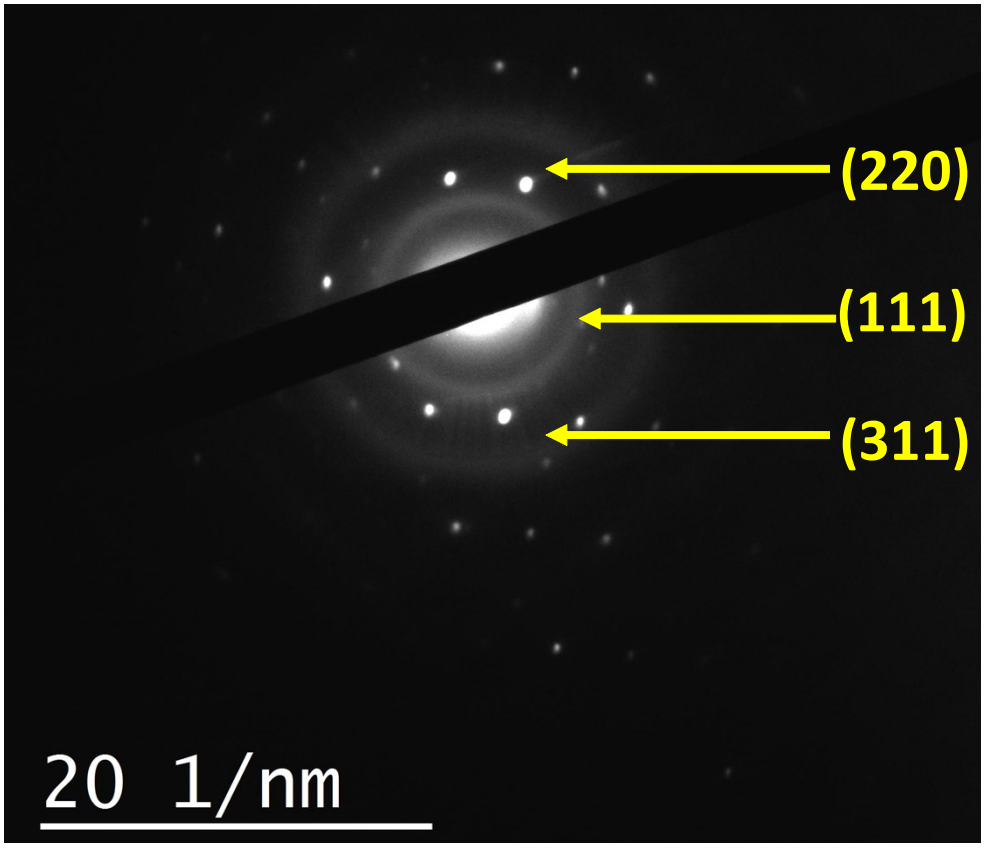

Fig. S8 Selected area electron diffraction pattern (SAED) of p-i-n SiNWs-NGQD.

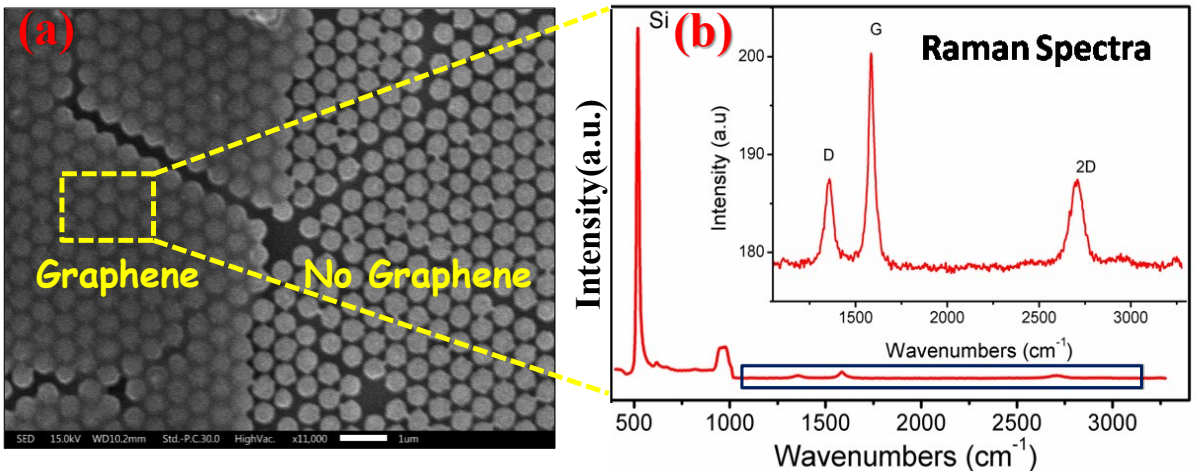

Fig. S9 (a) Top view of the graphene/SiNWs heterostructure. The darker blanket is the graphene sheet coated on the tip of SiNWs whereas the rest part is uncoated. (b) Raman spectra of few-layer graphene on SiNWs. The peak at 520 cm^{-1} is arising from the Si nanowires which corresponds to the scattering of incident light with the first-order optical phonon of the Si. Inset shows the magnified region of the rectangular box which refers to the characteristic peaks of the graphene floating on top of the vertical Si nanowires.

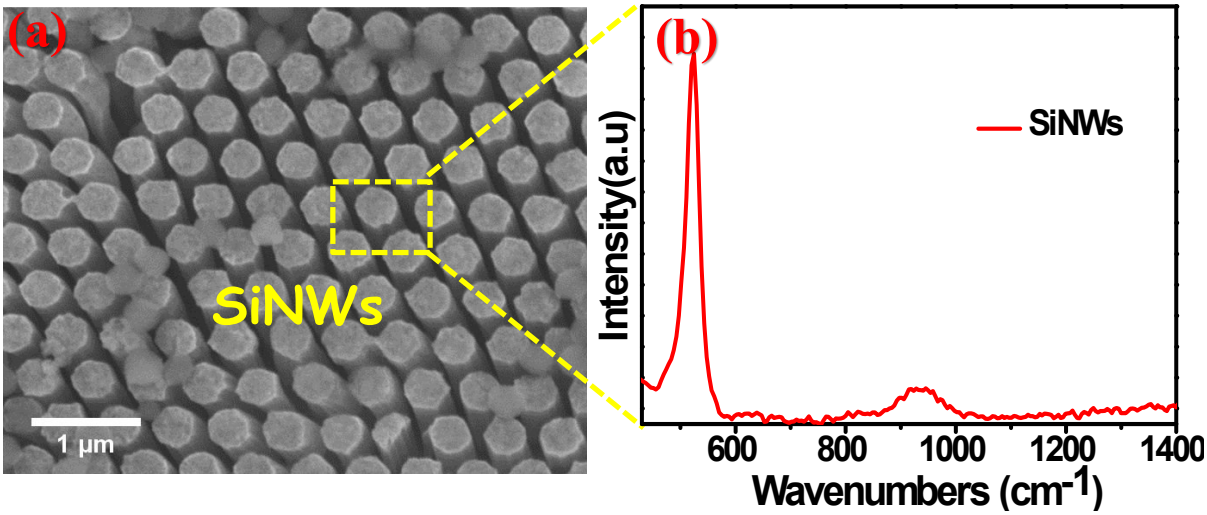

Fig. S10 (a) Top view of bare SiNWs. (b) Raman spectra of the corresponding SiNWs. The peak at 520 cm^{-1} is arising from the Si nanowires which corresponds to the scattering of incident light with the first-order optical phonon of the Si.

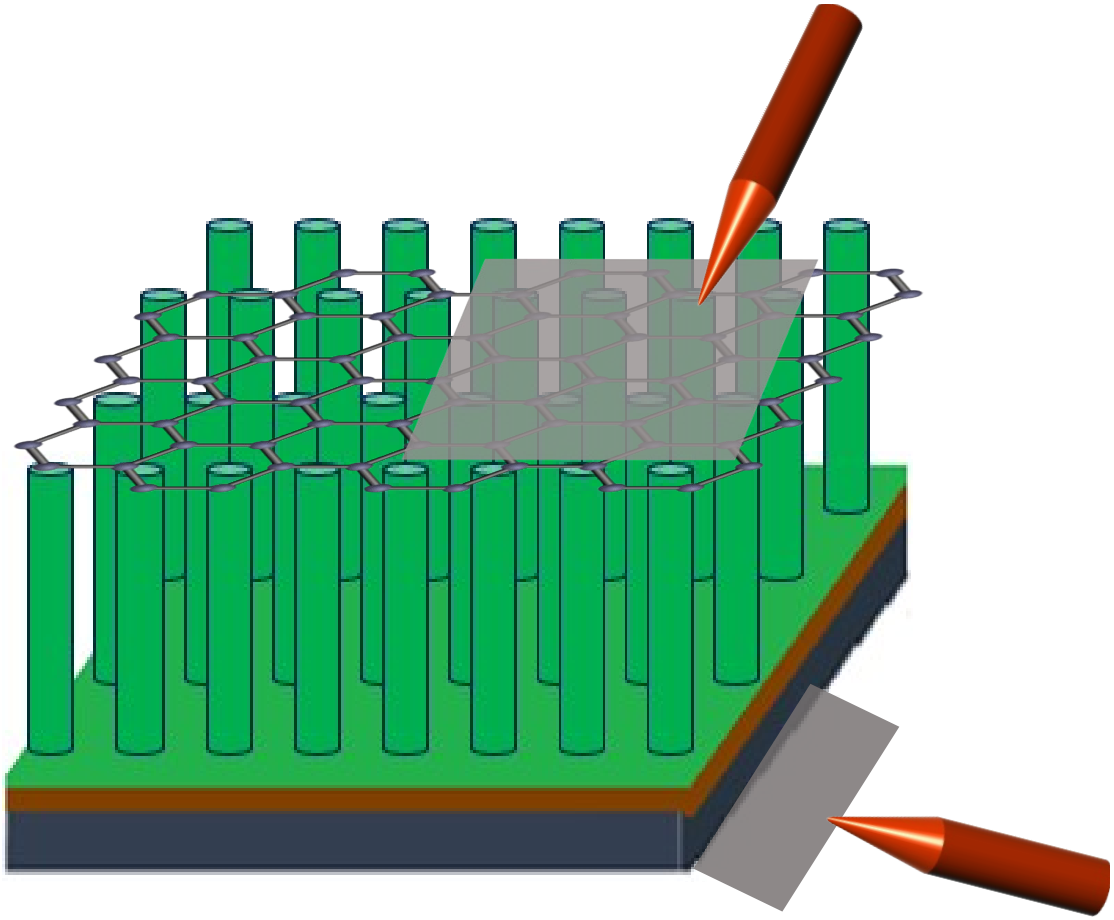

Fig. S11 Schematic illustration for the *I-V* measurement of SiNWs-graphene heterostructure

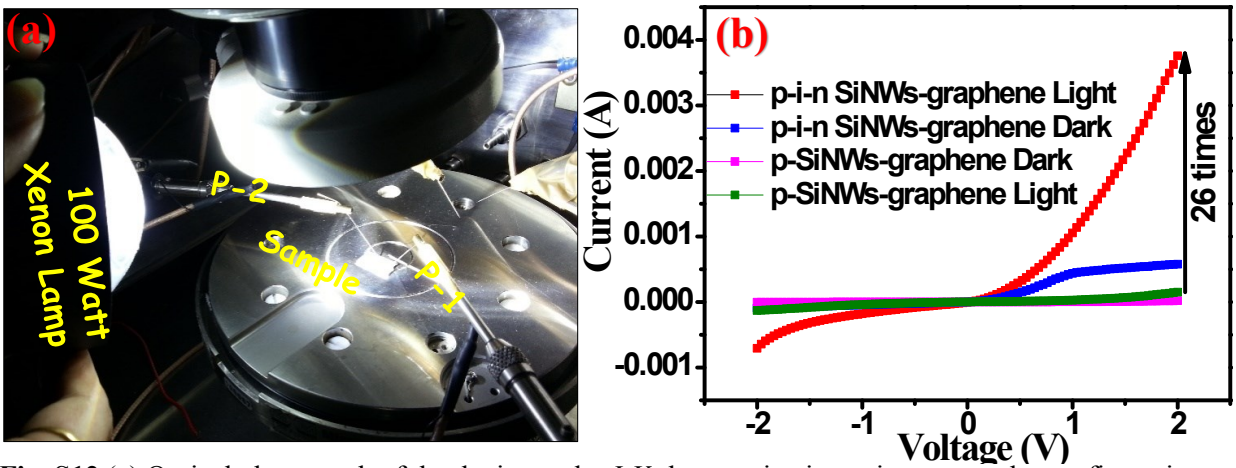

Fig. S12 (a) Optical photograph of the device under *I-V* characterization using two probe configuration by Keithley source meter (b) *I-V* measurement plots of p-SiNWs/graphene and p-i-n SiNWs/ graphene under light and dark condition.

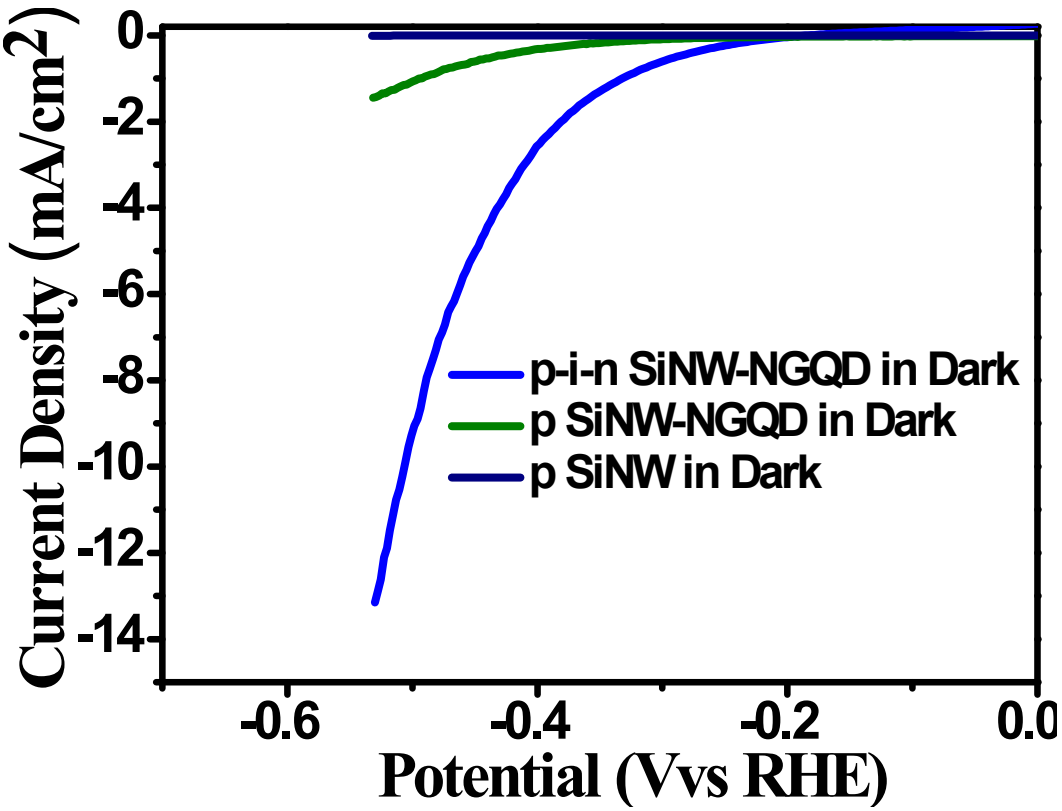

Fig. S13 LSV polarization curve (without *iR* correction) for p-SiNWs, p-SiNWs-NGQD and p-i-n SiNWs-NGQD in 0.5 M H_2SO_4 solution in dark condition.

Table S1. Shows comparison of PEC-HER performance in terms of onset, overpotential, photocurrent density and ABPE of all as-grown samples in 0.5 M H_2SO_4 solution under illuminated and dark conditions, respectively.

Condition	**Electrode**	**Onset potential (mV) @1mA/cm²**	**Overpotential (mV)@10mA/cm²**	**Current density (mA/cm²) @ -0.53V (*vs* RHE)**	**ABPE (%)**
Under illumination	p-SiNWs	-	-	-0.01	-
	p-SiNWs-NGQD	-411	-	-3.75	2.5
	p-i-n SiNWs-NGQD	-280	-460	-22.69	16.4
Under dark	p-SiNWs	-	-	-0.008	-
	p-SiNWs-NGQD	-492	-	-1.44	-
	p-i-n SiNWs-NGQD	-330	-505	-13.15	-

Hydrogen evolution reaction mechanism in acid medium:

Hydrogen evolution reaction proceeds *via* in three steps which undergoes two different reaction mechanisms where Volmer is the primary discharge step, common in both the mechanism. The mechanisms are Volmer-Heyrovsky and Volmer-Tafel. The three steps for hydrogen evolution are listed below.[1]

(1) $H_3O^+ + e^- + M \rightleftharpoons M\text{-}H_{ads} + H_2O$; Volmer reaction (discharge Step).

Here, electrons are moving towards the surface of the cathode and simultaneously hydronium ions (H_3O^+) which are coming from the electrolyte to form $M\text{-}H_{ads}$ intermediate state (Here M is the active surface of the metal). In this step Tafel slope b ~ 120 mV.

(2) $M\text{-}H_{ads} + H_3O^+ + e^- \rightleftharpoons H_2 + M + H_2O$; Heyrovsky reaction (desorption step).

When the density of H_{ads} on the metal surface is very less, the H_{ads} intermediates combine with the new electron and hydronium ion and produce H_2 molecule; In this step Tafel slope, b ~ 40 mV.

(3) $M\text{-}H_{ads} + H_{ads}\text{-}M \rightleftharpoons H_2 + 2M$; Tafel reaction (Recombination Step).

When the density of H_{ads} on the metal surface is high, the two nearby H_{ads} intermediates combine together and produce H_2 molecule. Tafel slope b ~ 30 mV.

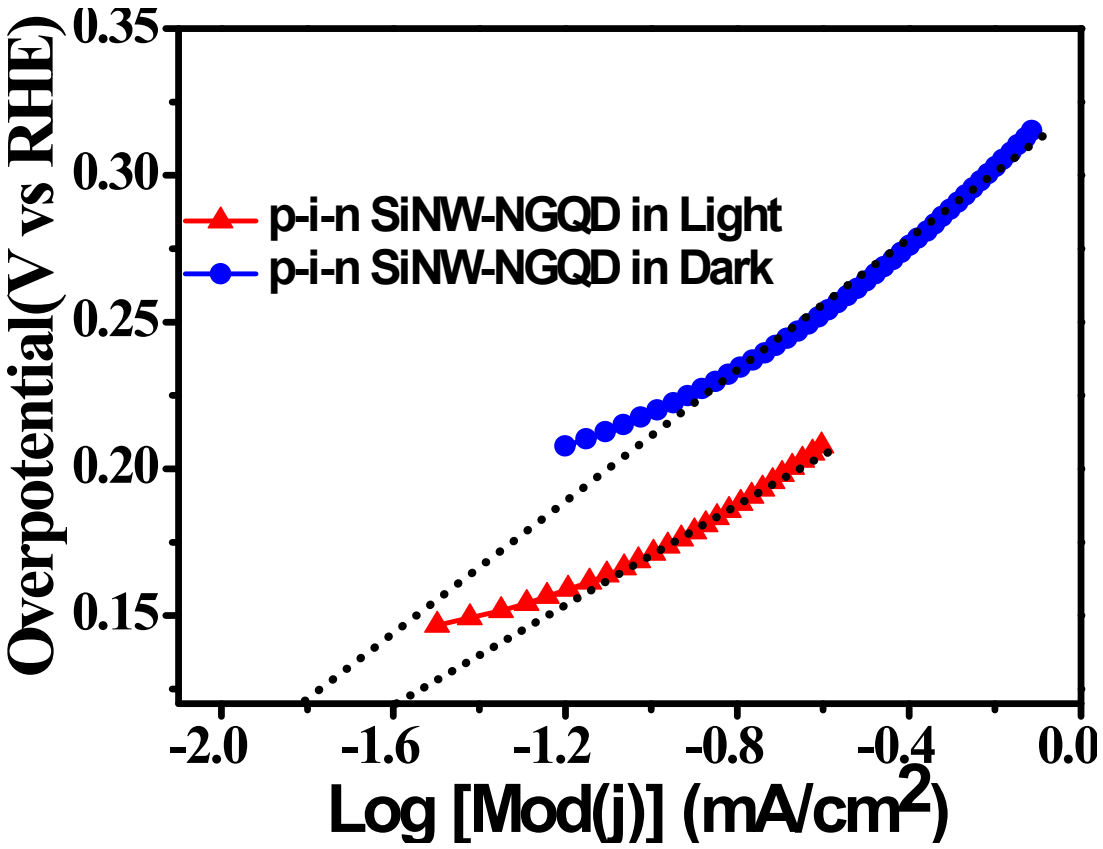

Fig. S14 The exchange current density of p-i-n SiNWs-NGQD are calculated to be 0.026, 0.015 mA/cm^2 in p-i-n SiNWs-NGQD in light and dark condition, respectively *via* extrapolating the Tafel plots to the X-axis.

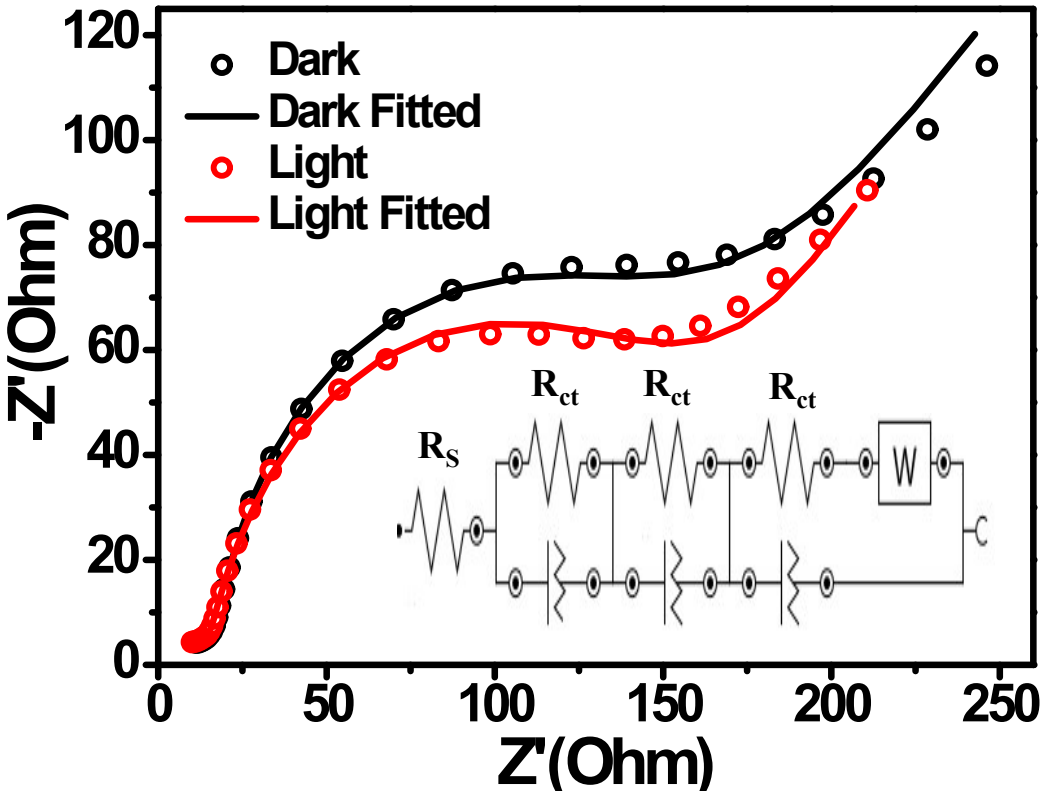

Fig. S15 Nyquist plots of p-i-n SiNWs-NGQD in light and dark conditions at an applied potential of -300 mV in 0.5 H_2SO_4 solution. Inset shows the fitted circuit diagram of the above Nyquist plots.

Table S2. The PEC-HER performance of the as-prepared p-i-n SiNWs-NGQD heterostructure in comparison with the recently reported Metal and Metal-Free Si-based photocathodes.

Si with Metal-Based HER							
Sr. No.	**Material**	**Electrolyte**	**Photocurrent (mA/cm^2)**	**ABPE (%)**	**Tafel (mV/dec)**	**Overpotential (mV) @10mA/cm²**	**Ref.**
1.	Si-$SrTiO_3$ (Ti/Pt catalyst)	0.5M H_2SO_4	-35	4.9	-	-	[2]
2.	Si /Al_2O_3 (Pt catalyst)	0.5M H_2SO_4	-26.2	-	-	-	[3]
3.	Si /Au /Pt Si/Pt NP Si/Au NF	0.5MH_2SO_4+ 0.5MK_2SO_4	-24.4 -26.6 -24.5	-	56	-71 -78 -120	[4]
4.	Si / MoS_2	0.5M H_2SO_4	-17.6		-	-	[5]
5.	Si/TiO_2/ MoS_2	0.5 M H_2SO_4	-37	1.8%	87.01	-255	[6]
6.	n^+p-Si/$MoSe_2$	1 M $HClO_4$	-29.3	3.8%	-	-195	[7]
7.	Si/TaO_x	1 M HCl	-37.1	7.7%	-	-	[8]
8.	Si/MoS_2Cl	0.5MH_2SO_4	-20.6	-	46	-	[9]
9.	p-Si/SiO_2/Ti/Pt	0.5 M H_2SO_4	-22	2.9%	-	-	[10]
10.	n^+p Si-Ti-MoS_x	1M $HclO_4$	-12	-	-	-	[11]
11.	n^+p-Si /TiO_2/Pt	1M $HclO_4$	-34.8	STH-10.8	35	-	[12]
12.	n^+p Si/Mo/MoS_2/Pt n^+pSi/Mo/MoS_2/MoS_x/Pt n^+p-Si/W/WS_2/Pt	1.0 M $HclO_4$	-10.9 -12 -9	- - -	36	-	[13]
13.	n^+p-Si/Co-S	0.5M H_2SO_4	-11	-	104	-85	[14]
14.	n-Si/SiO_x,/Al_2O_3/Pt/Ni	1M KOH	-28.5	-	-	-	[15]
15.	SiNW/Ni-B SiNW/Co-B	2M Phosphate buffer solution	-15.6 -19.5	2.45 2.53	-	-54	[16]
16.	p-Si NW/Pt	H_2SO_4 + 0.5M K_2SO_4 (pH=1)	-20	-	-	-	[17]
17.	p-SiNWs/TiO_2/Pt	0.5M H_2SO_4	-30	-	-	-	[18]
18.	p-SiNWs/MoS_2	1M Na_2SO_4	-1	STH-0.03%	-	-	[19]

19.	n-SiNWs/Ba_2O_3	1m NaOH	-3.5	0.47%	-	-	[20]
20.	SiNWs/CdSe QD	0.25M Na_2S + 0.35M Na_2SO_3	-6.1	-	-	-	[21]
21.	Si/PEDOT hybrid core/shell NW array	1M KOH	-2.5	-	-	-	[22]
22.	Si/ZnO wires/IrOx QDs	Na_2S+Na_2SO_3	-1.64	0.55%	-	-	[23]
23.	n^+ p-Si wires/Pt	0.1M K_2SO_4+ H_2SO_4	-15	5.8	-	-	[24]
24.	n^+ p-Si single NWs/Pt	H_2SO_4 + 0.1M K_2SO_4 (pH=2)	-22	-	-	-	[25]
25.	n^+p Si microwire /Ni-Mo n^+p Si microwire/Pt	KHP Buffer (pH=4)	-9.1 -13.2	1.9 (STH) 2.7 (STH)	-	-	[26]
26.	SiNW/ $Fe_2S_2(CO)_6$	0.1M H_2SO_4	-17	-	-	-	[27]
27.	Vertically aligned SiNWs (n-type)	200mM Me_2FcB_4 + 1M $LiClO_4$ in Ethanol.	-4.19	-	-	-	[28]
28.	Mo_3S_4/p- Si	1M $HClO_4$	-9	STH-10%	-	-400	[29]
29.	Si MWs/MoO_xS_y -10 Si MWs/MoO_xS_y -30 Si MWs/MoO_xS_y -50	0.5M K_2SO_4 + H_2SO_4	-1.28 -7.35 - 9.83	STH-0.05 0.63 0.82	-	-	[30]
30.	Si MWs/$CoSe_2$	0.5 M Na_2SO_4 / H_2SO_4 ,	-9	STH-0.93	-	-	[31]
31.	Si NWs/$Ni_{12}P_5$ Si NWs/Ni_2P	0.5 M H_2SO_4	-21 -22.6	STH-2.97 STH-3.13	63	-107	[32]

32.	Si NWs/Co-P	0.5M K_2SO_4 /H_2SO_4	-15.6	STH-2.86	-	-	[33]
33.	Si NWs/FeP	0.5M K_2SO_4 /0.05M H_2SO_4	-13.9	STH-2.64	-	-	[34]
34.	Si MWs/CoS_2 Si MWs/$CoSe_2$	0.5M H_2SO_4 1.0 M PBS	-3.22 -2.55	- -	62.8 39.5	-	[35]
35.	Si NWs/MoS_3	0.5 M K_2SO_4 + H_2SO_4	-24.9	STH-2.28	-	-	[36]
36.	Si NWs/MoS_3	0.5 M K_2SO_4 + H_2SO_4	-1.5	-	-	-	[37]
37.	Si wires/WS_3 Si wires/WS_2	0.5M K_2SO_4/0.05 M H_2SO_4	-19 -7	STH-2.02 STH-0.187	-	-	[38]
38.	a-Si /Mo_2C	0.1 M H_2SO_4 1 M KOH	-11.2 -11.4	- -	56 54	-270	[39]
39.	p-i-n Si/ Pt/Co_3O_4 n-i-p/ Si Pt/Co_3O_4	1M KOH 1M KOH	-12.03 -7.3	3.3 0.93	-	-	[40]

Metal-Free Si based HER							
1.	Graphene/Si	1M $HClO_4$	-31.1	0.32	-		[41]
2.	SiNW@N-doped GQS	1M $HClO_4$	-35	2.29	45	-	[42]
3.	N-doped monolayer Graphene/ Silicon	1M $HClO_4$	-5.5	STH-3.05	-	-	[43]
4.	rGO-SiNWs	1M $HClO_4$	-23.152	STH-3.16	45	-	[44]
5.	Chl/CQDs-SiNWs	0.5M H_2SO_4	-26.36	7.86	-	-	[45]
6.	**p-i-n SiNWs/NGQD**	**0.5 M H_2SO_4**	**-26.2**	**16.4**	**46**	**-460**	**Our work**

[#]ABPE- Applied Bias Photon-to-Current Efficiency

[#]STH- Solar to Hydrogen Conversion Efficiency

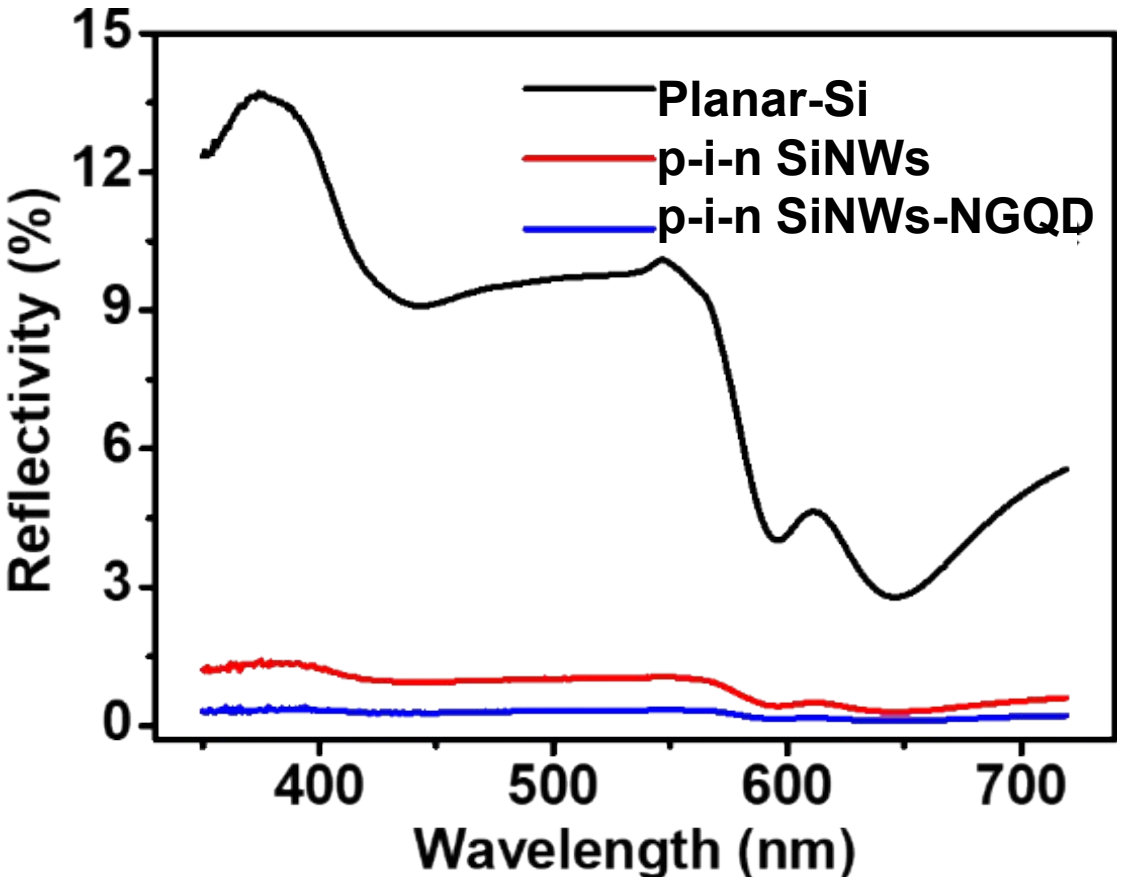

Fig. S16 UV-Vis analysis of Planar Si, p-i-n SiNWs and the p-i-n SiNWs-NGQD hetero-structure. The result shows that p-i-n-SiNWs and the p-i-n SiNWs-NGQD hetero-structure reflects 89.5% and 96.65% less light as compared to planar Si substrate in the visible range of solar spectra.

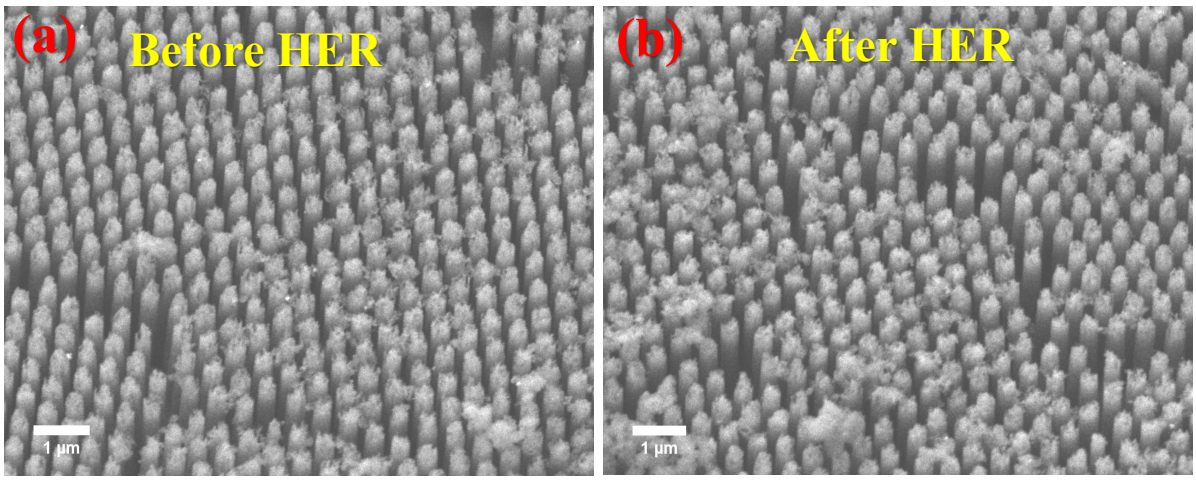

Fig. S17 FE-SEM images of p-i-n SiNWs-NGQD (a) before and (b) after stability test refer to no significant change in morphology of catalyst has been observed.

References:

1. S. Riyajuddin, K. Azmi, M. Pahuja, S. Kumar, T. Maruyama, C. Bera and K. Ghosh, *ACS Nano*, , DOI:10.1021/acsnano.1c00647.
2. L. Ji, M. D. McDaniel, S. Wang, A. B. Posadas, X. Li, H. Huang, J. C. Lee, A. A. Demkov, A. J. Bard, J. G. Ekerdt and E. T. Yu, *Nature Nanotechnology*, 2015, **10**, 84–90.
3. M. J. Choi, J.-Y. Jung, M.-J. Park, J.-W. Song, J.-H. Lee and J. H. Bang, *J. Mater. Chem. A*, 2014, **2**, 2928–2933.
4. J. Kye, M. Shin, B. Lim, J.-W. Jang, I. Oh and S. Hwang, *ACS Nano*, 2013, **7**, 6017–6023.
5. Q. Ding, F. Meng, C. R. English, M. Cabán-Acevedo, M. J. Shearer, D. Liang, A. S. Daniel, R. J. Hamers and S. Jin, *J. Am. Chem. Soc.*, 2014, **136**, 8504–8507.
6. D. M. Andoshe, G. Jin, C.-S. Lee, C. Kim, K. C. Kwon, S. Choi, W. Sohn, C. W. Moon, S. H. Lee, J. M. Suh, S. Kang, J. Park, H. Heo, J. K. Kim, S. Han, M.-H. Jo and H. W. Jang, *Adv. Sustainable Syst.*, 2018, **2**, 1700142.
7. G. Huang, J. Mao, R. Fan, Z. Yin, X. Wu, J. Jie, Z. Kang and M. Shen, *Appl. Phys. Lett.*, 2018, **112**, 013902.
8. Y. Wan, S. K. Karuturi, C. Samundsett, J. Bullock, M. Hettick, D. Yan, J. Peng, P. R. Narangari, S. Mokkapati, H. H. Tan, C. Jagadish, A. Javey and A. Cuevas, *ACS Energy Lett.*, 2018, **3**, 125–131.
9. X. Zhang, F. Meng, S. Mao, Q. Ding, M. J. Shearer, M. S. Faber, J. Chen, R. J. Hamers and S. Jin, *Energy Environ. Sci.*, 2015, **8**, 862–868.
10. D. V. Esposito, I. Levin, T. P. Moffat and A. A. Talin, *Nature Materials*, 2013, **12**, 562–568.
11. B. Seger, A. B. Laursen, P. C. K. Vesborg, T. Pedersen, O. Hansen, S. Dahl and I. Chorkendorff, *Angewandte Chemie International Edition*, 2012, **51**, 9128–9131.
12. R. Fan, W. Dong, L. Fang, F. Zheng and M. Shen, *J. Mater. Chem. A*, 2017, **5**, 18744–18751.
13. A. B. Laursen, T. Pedersen, P. Malacrida, B. Seger, O. Hansen, P. C. K. Vesborg and I. Chorkendorff, *Phys. Chem. Chem. Phys.*, 2013, **15**, 20000–20004.
14. Y. Sun, C. Liu, D. C. Grauer, J. Yano, J. R. Long, P. Yang and C. J. Chang, *J. Am. Chem. Soc.*, 2013, **135**, 17699–17702.
15. I. A. Digdaya, G. W. P. Adhyaksa, B. J. Trześniewski, E. C. Garnett and W. A. Smith, *Nature Communications*, 2017, **8**, 15968.
16. Y. Yang, M. Wang, P. Zhang, W. Wang, H. Han and L. Sun, *ACS Appl Mater Interfaces*, 2016, **8**, 30143–30151.
17. I. Oh, J. Kye and S. Hwang, *Nano Lett.*, 2012, **12**, 298–302.
18. N. P. Dasgupta, C. Liu, S. Andrews, F. B. Prinz and P. Yang, *J Am Chem Soc*, 2013, **135**, 12932–12935.
19. P. D. Tran, S. S. Pramana, V. S. Kale, M. Nguyen, S. Y. Chiam, S. K. Batabyal, L. H. Wong, J. Barber and J. Loo, *Chemistry*, 2012, **18**, 13994–13999.
20. B. Weng, F. Xu and J. Xu, *Nanotechnology*, 2014, **25**, 455402.
21. R. R. Devarapalli, C. K. Kamaja and M. V. Shelke, *J. Mater. Chem. A*, 2014, **2**, 13352–13358.
22. X. Li, W. Lu, W. Dong, Q. Chen, D. Wu, W. Zhou and L. Chen, *Nanoscale*, 2013, **5**, 5257–5261.
23. W. Sheng, B. Sun, T. Shi, X. Tan, Z. Peng and G. Liao, *ACS Nano*, 2014, **8**, 7163–7169.
24. S. W. Boettcher, E. L. Warren, M. C. Putnam, E. A. Santori, D. Turner-Evans, M. D. Kelzenberg, M. G. Walter, J. R. McKone, B. S. Brunschwig, H. A. Atwater and N. S. Lewis, *J. Am. Chem. Soc.*, 2011, **133**, 1216–1219.

25.Y. Su, C. Liu, S. Brittman, J. Tang, A. Fu, N. Kornienko, Q. Kong and P. Yang, *Nat Nanotechnol*, 2016, **11**, 609–612.
26.E. L. Warren, J. R. McKone, H. A. Atwater, H. B. Gray and N. S. Lewis, *Energy Environ. Sci.*, 2012, **5**, 9653–9661.
27.S. Chandrasekaran, T. Nann and N. H. Voelcker, *Nanomaterials*, 2016, **6**, 144.
28.G. Yuan, H. Zhao, X. Liu, Z. S. Hasanali, Y. Zou, A. Levine and D. Wang, *Angewandte Chemie International Edition*, 2009, **48**, 9680–9684.
29.Y. Hou, B. L. Abrams, P. C. K. Vesborg, M. E. Björketun, K. Herbst, L. Bech, A. M. Setti, C. D. Damsgaard, T. Pedersen, O. Hansen, J. Rossmeisl, S. Dahl, J. K. Nørskov and I. Chorkendorff, *Nature Materials*, 2011, **10**, 434–438.
30.X.-Q. Bao, D. Y. Petrovykh, P. Alpuim, D. G. Stroppa, N. Guldris, H. Fonseca, M. Costa, J. Gaspar, C. Jin and L. Liu, *Nano Energy*, 2015, **16**, 130–142.
31.M. Basu, Z.-W. Zhang, C.-J. Chen, P.-T. Chen, K.-C. Yang, C.-G. Ma, C. C. Lin, S.-F. Hu and R.-S. Liu, *Angewandte Chemie International Edition*, 2015, **54**, 6211–6216.
32.Z. Huang, Z. Chen, Z. Chen, C. Lv, H. Meng and C. Zhang, *ACS Nano*, 2014, **8**, 8121–8129.
33.X.-Q. Bao, M. F. Cerqueira, P. Alpuim and L. Liu, *Chem. Commun.*, 2015, **51**, 10742–10745.
34.C. Lv, Z. Chen, Z. Chen, B. Zhang, Y. Qin, Z. Huang and C. Zhang, *J. Mater. Chem. A*, 2015, **3**, 17669–17675.
35.C.-J. Chen, K.-C. Yang, M. Basu, T.-H. Lu, Y.-R. Lu, C.-L. Dong, S.-F. Hu and R.-S. Liu, *ACS Appl Mater Interfaces*, 2016, **8**, 5400–5407.
36.Z. Huang, C. Wang, L. Pan, F. Tian, X. Zhang and C. Zhang, *Nano Energy*, 2013, **2**, 1337–1346.
37.G.-L. Zang, G.-P. Sheng, C. Shi, Y.-K. Wang, W.-W. Li and H.-Q. Yu, *Energy Environ. Sci.*, 2014, **7**, 3033–3039.
38.Z. Huang, C. Wang, Z. Chen, H. Meng, C. Lv, Z. Chen, R. Han and C. Zhang, *ACS Appl. Mater. Interfaces*, 2014, **6**, 10408–10414.
39.C. G. Morales-Guio, K. Thorwarth, B. Niesen, L. Liardet, J. Patscheider, C. Ballif and X. Hu, *J Am Chem Soc*, 2015, **137**, 7035–7038.
40.D. Zhang, Y. Cao, S. K. Karuturi, M. Du, M. Liu, C. Xue, R. Chen, P. Wang, J. Zhang, J. Shi and S. F. Liu, *ACS Appl. Energy Mater.*, 2020, **3**, 4629–4637.
41.U. Sim, J. Moon, J. Lee, J. An, H.-Y. Ahn, D. J. Kim, I. Jo, C. Jeon, S. Han, B. H. Hong and K. T. Nam, *ACS Appl. Mater. Interfaces*, 2017, **9**, 3570–3580.
42.U. Sim, J. Moon, J. An, J. H. Kang, S. E. Jerng, J. Moon, S.-P. Cho, B. H. Hong and K. T. Nam, *Energy Environ. Sci.*, 2015, **8**, 1329–1338.
43.U. Sim, T.-Y. Yang, J. Moon, J. An, J. Hwang, J.-H. Seo, J. Lee, K. Y. Kim, J. Lee, S. Han, B. H. Hong and K. T. Nam, *Energy Environ. Sci.*, 2013, **6**, 3658–3664.
44.Y. Sim, J. John, J. Moon and U. Sim, *Applied Sciences*, 2018, **8**, 2046.
45.K. Roy, D. Ghosh, K. Sarkar, P. Devi and P. Kumar, *ACS Appl. Mater. Interfaces*, 2020, **12,** 37218–37226.